Assessment of the polarizabilities (α, β) of a nonlinear optical compound [*N*-(4-nitrophenyl)-(*L*)-prolinol] from an experimental electronic density study

Abdallah Fkyerat, Abdelhalim Guelzim, and François Baert*
Laboratoire de Dynamique et Structure des Matériaux Moléculaires, CNRS URA 801, Université des Sciences et Technologies de Lille Flandres Artois, 59655 Villeneuve d'Ascq Cédex, France

Joseph Zyss and A. Périgaud
Département d'Electronique Quantique et Moléculaire, Laboratoire de Bagneux, (CNET), 196 Avenue Henri Ravera, 92220 Bagneux, France

(Received 12 September 1995; revised manuscript received 29 January 1996)

The underlying ambition of this work in addition to the x-ray diffraction electronic density determination is the estimation of the nonlinear optical properties of NPP [*N*-(4-nitrophenyl)-(*L*)-prolinol] from a model due to Robinson allowing us to connect the polarizabilities, under some approximations, to the different multipolar moments of the electronic charge distribution. The calculations of the atomic net charges demonstrate the character of the donor-acceptor (DA) pair linked to the phenyl transmitter. The dipolar molecular moments obtained by several methods have similar values, except the one from the κ method. This analysis suggests that aspherical pseudoatoms are essential for modeling the charge distribution in a noncentrosymmetric crystal. The validity of the Unsöld approximation, using the results obtained by a semiempirical method implemented in the electronic part of MOPAC (AM1 Hamiltonian), have been evidenced. The Unsöld approximation gives relatively good results for α but falls off by two orders of magnitude in the estimation of β. The results from the experimental electronic density study indicate that there is some added fluctuation in the modulus of the components, with respect to those derived from the so-called point charge model, but the signs are in good agreement. Those fluctuations are certainly related to the molecular interactions, which screen to some extent the nonlinear efficiency of the molecule. [S0163-1829(96)03124-4]

INTRODUCTION

Interest in nonlinear optics has grown tremendously in recent years, due to applications as well as fundamental motivations and has centered around the unusually large nonlinear second-order optical susceptibilities of organic solids and polymers.[1] These materials are generally composed of dipolar aromatic molecules that are substituted with π electrons, donor and acceptor, and exhibit intramolecular charge transfer between the two groups. Among such systems, paranitroaniline derivatives stand out as a class of prototype organic molecules for second-harmonic generation (SHG). Second-harmonic generation in *N*-(4-nitrophenyl)-*L*-prolinol (NPP) is, for instance, two orders of magnitude larger than in KTP, the state of the art in nonlinear inorganic crystal.

Since the second-order hyperpolarizability (β) of such molecules is at the origin of SHG, extensive studies have been performed towards the theoretical estimation of β using either semiempirical PPP-molecular orbital,[2–4] complete neglect of differential overlap 1S,[5–9] INDO (Ref. 10) or *ab initio*[11–13] molecular orbital calculations.

In general, however, the net SHG property in an organic material results from a combination of both the electronic property of an isolated molecule associated with β (e.g., a conjugated π electron system with intramolecular charge transfer) and the crystalline assembly with various intermolecular interactions coupling individual molecular units of steric, structural, or electromagnetic natures (H-bond, etc.).

Indeed calculated β values very often reveal discrepancies from net SHG effects observed by powder-method measurements, mostly as a consequence arising from the ignorance of hydrogen bonds, cancellation of unfavorably orientated molecular optical dipoles, and unknown local field effects in the crystalline state. Robinson,[14] Flytzanis and Ducuing,[15] and Jha and Bloembergen[16] showed through simplifying models or approximations (Unsöld,[17]) and far from resonances,that susceptibilities were connected to the various moments of the charge distribution in the ground state.

Following this development, we concentrate on the molecular properties, namely, the molecular quadrupolar and octupolar moments, calculated by integrating the electronic density distribution obtained by an accurate x-ray diffraction study.

In parallel, the above properties were deduced from a semiempirical calculation using MOPAC (Ref. 18) (AM1,PM3), were the positional parameters of the atoms are inferred from x-ray crystallographic analysis. Values of polarizability and hyperpolarizability tensors for the molecule were also obtained using the finite field method.[19] These estimates at the molecular level are compared to assess the validity of the Unsöld approximation, which relates multipolar moments of the ground-state charge distribution to linear and nonlinear hyperpolarizabilities.

Since the development of sufficiently compact parametrized descriptions of molecular densities, about twenty years ago, accurate experimental measurement of the charge density in a crystal has been shown to be feasible.[20] After the

TABLE I. Experimental data for *N*-(4-nitrophenyl)-*L*-prolinol.

Parameter	X-ray	Neutrons
a (Å)	5.152(4)	5.164(2)
b (Å)	14.790(3)	14.796(8)
c (Å)	7.134(2)	7.108(5)
β (deg)	106.14(4°)	105.86 (3°)
Space group	$P2_1$	$P2_1$
T (K)	122 K (0.5°)	122 K (2°)
λ (Å)	0.7107	0.8308
$(\sin\theta/\lambda)$ max (Å^{-1})	1.153	0.774
Measured reflections	8424	2086
(hkl regions)	$\pm H \pm K + L$	$\pm H \pm K + \pm L$
Unique reflections	3807	1472
$R_{\text{int}(\pm)}$	0.014	0.047
Absorption correction	no	yes
Number of variables	145	271
${}_aR\omega$ (F)	0.044	0.031
${}_bR\omega$ (F^2)	0.089	0.062
μ (cm^{-1})	0.846	1.4
Extinction correction	no	yes
Mosaïc spread		221(15)″ arc
Extinction factor $y = (F_0^2/F_{\text{corr}}^2)$ less than 0.9		y_{120},0.88;y_{101},0.76;y_{021},0.88

$$ {}_aR_\omega(F) = \left\{ \frac{\sum_w |F_0 - kF_c|^2}{\sum_w F_0^2} \right\}^{1/2} \qquad {}_bR_\omega(F^2) = \left\{ \frac{\sum_w |F_0^2 - k^2F_c^2|^2}{\sum_w F_0^4} \right\}^{1/2} $$

appearance of the pioneer paper of Coppens *et al.*,[21] a great number of studies in this field have demonstrated the feasibility of accessing by advanced diffraction experiments to the electron density determination and the outer moments of the charge distribution for a centrosymmetic molecular crystal. Applications of such an analysis to noncentrosymmetric materials, such as organic nonlinear optical compounds, have been slow to emerge, the main reason being the difficulties of solving the phase problem. However, recent applications using the multipolar development of the charge density around the atoms, which constitutes the molecule, have shown the potential accuracy of the technique in the noncentrosymmetric case.[22]

From such a study it is, for instance, possible to access to the octupole moment of the molecular electronic distribution in the crystal state, which is connected to the components of the β tensor (Robinson[14]). An estimation of the β_{ijk} components is of primary importance for the evaluation of the efficiency of the nonlinear properties of the material.

EXPERIMENTAL DETAILS

Synthesis and crystal growth

Yellow crystals of NPP,[23] crystallized during the Crocodile space experiment (Perigaud, Gonzales, and Cunisse[24]) have been provided by the CNET. A crystal from the reduced gravity experiment of $0.45\times0.32\times0.21$ mm^3 in size was used in the x-ray diffraction experiment. Single NPP crystals, even of small size, are difficult to obtain. Gel growth techniques[25] have also been attempted to grow highly nonlinear NPP crystals of larger size.

X-ray structure investigation

Single crystal x-ray diffraction experiments were carried out on an Enraf-Nonius CAD4 diffractometer, using Mo $K\alpha$ radiation from a graphite monochromator. A measuring temperature of 122 K was established by means of an Enraf-Nonius nitrogen cool gas device. The temperature fluctuation was estimated to be of the order of $\pm$ 0.5° during data collection. Cell parameters were determined from refinement, using centered angular positions of 25 reflections with $25° < 2\theta < 35°$. The homogeneity of the beam from the graphite incident beam monochromator was measured with a pinhole of 20 micrometers, and the intensity varied by less than 3.5% over the area intercepted by the specimen crystal. Measurements covered half a sphere with $-10 < H < 10$, $-34 < K < 34$, $0 < L < 15$.

During the data collection, five standard reflections were measured every two hours. Data reduction and error analysis were carried out using the programs of Blessing.[26] Reflection integration limits were taken from a Lorentzian model for peak-width variations. A polynomial fit to the smooth decline of $\sim$ 0.03% in the standard reflection intensities over

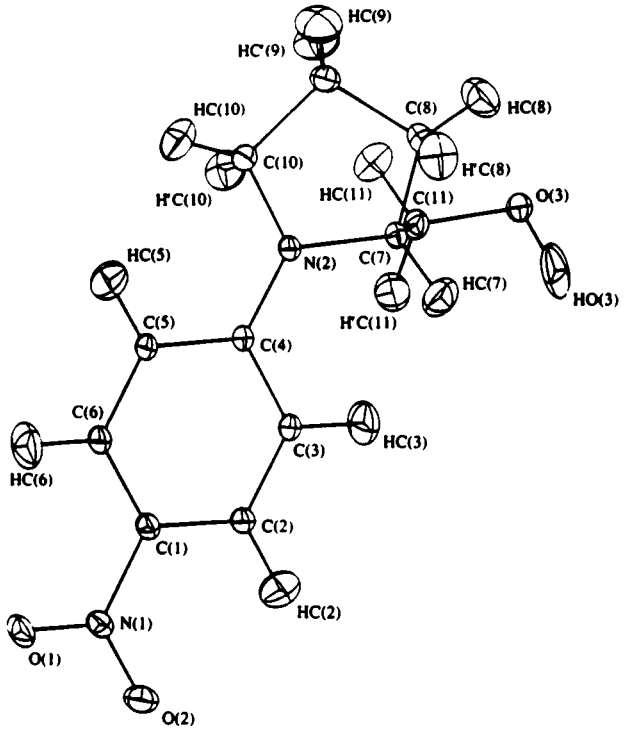

FIG. 1. Ortep diagram of the NPP molecule. Debye-Waller factors have been calculated from $TLS+\phi$ + group tensors of the internal vibrations. Thermal ellipsoids are at the 30% probability level.

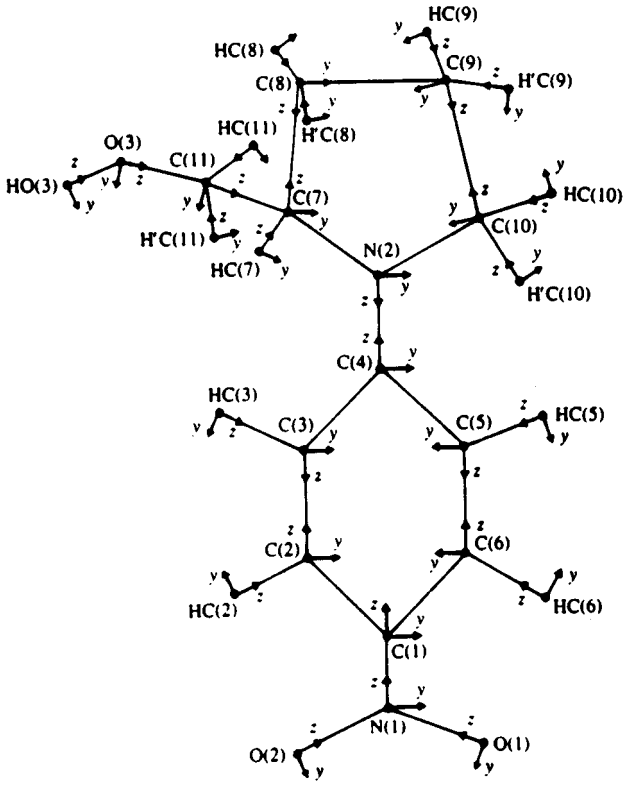

FIG. 2. Labeling of the atoms and definition of local orthogonal reference axes for the atom-centered multipolar functions.

the three weeks of x-ray exposure was used to scale the data. Absorption and beam-inhomogeneity corrections were not neccessary. No $\sigma(I)/I$ rejection criteria was applied to the x-ray data. The x-ray diffraction experiment was completed by neutron diffraction measurements at the same temperature.[27] Table I summarizes the physical parameters for the two experiments.

All refinements done in this study used the rigid pseudoatom model of Hansen and Coppens.[28] The electron density $\rho(r)$ in the crystal is described by a sum of the so-called aspherical ''pseudoatoms,'' with nuclear positions r_k:

$$\rho(\vec{r})=\sum_k \rho_k(\vec{r}-\vec{r}_k-\vec{u})\star t_k(\vec{u}), \tag{1}$$

where $t_k(\vec{u})$ is a Gaussian thermal-displacement distribution and $\star$ indicates a convolution product.

Each atomic density is described as a series expansion in real spherical harmonic functions ($Y_{lm^+_-}$), up to the fourth order:

$$\rho_k(\vec{r})=P_{k,c}\rho_{k,c}(\vec{r})+P_{k,v}\kappa^3\rho_{k,v}(\kappa,r) + \sum_{l=0}^{4}\kappa'^3 R_{k,l}(\kappa',r)\sum_{m=0}^{l} P_{lm^+_-}Y_l m^{\pm}_{-}\left(\frac{\vec{r}}{|r|}\right). \tag{2}$$

The sum over m in Eq. (2) includes $\pm$, so that for each l, $2l+1$ functions are included. In Eq. (2), ρ_c and ρ_v are the spherically averaged Hartree-Fock core and valence densities, with ρ_v normalized to one electron. The Slater type radial functions $R_l=N_l r^n\exp(-\kappa'\zeta r)$ are modulated by the multipolar spherical harmonic angular functions $Y_{lm\pm}$ and N_l is a normalization factor. The values for parameters $n=n_l$ and ζ were chosen according to rules provided by Hansen and Coppens:[28] $n_l=2,2,3,4$ and $\zeta_l=2.8$, 4.0, 5.06 (Å^{-1}) for C, O, N were used, respectively, for $l=1,2,3,4$. For the H atoms $n_l=2$ and $\zeta_l=2.0$ for $l=1,2$. The ζ_l parameters were free to vary during the refinement.

The adjustable variables are the valence shell contraction-expansion parameters κ and κ' and the population parameters P_v and $P_{lm\pm}$. To reduce the number of variables, chemical constraints were imposed on the multipole parameters: atoms of similar environment were assumed to have the same deformation. Local pseudoatom coordinate systems are defined in Fig. 2. Figure 1 shows an Ortep diagram of the NPP molecule, where ellipsoids represent the thermal motion of the atoms.

The multipolar refinements, which provide quantitative results, are generally used to complete the more qualitative $X-X_{HO}$ or $X-X_N$ studies. Since the structure of the quadratic NLO compounds are noncentrosymmetric, the multipolar procedure here is essential to evaluate the phases of the structure factors in order to get reliable electron density maps and one electron properties. Recent applications by Souhassou, Lecomte, Blessing, Aubry, Rohmer, Wiest, and Benard[22] have demonstrated the usefulness and the potential accuracy of the method. Figure 3 shows the distribution of $2|F_s|\sin(\Delta\phi/2)$ as a function of $\sin\theta/\lambda$ and $|F|$. F_s is the structure factor calculated by the spherically averaged free-atom superposition model. As expected, due to the highly

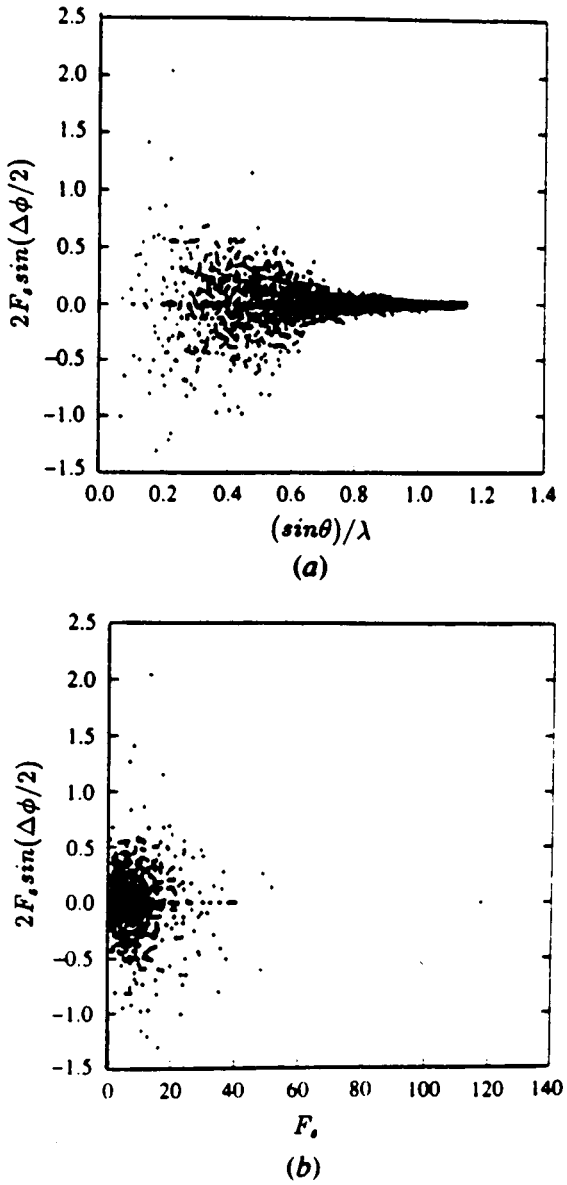

FIG. 3. Distribution of $2F\sin(\Delta\phi/2)$ (in units of electrons) against (a) $(\sin\theta/\lambda)$ and (b) $|F|$.

diffuse distribution of the valence electron, $2|F_s|\sin(\Delta\phi/2)$ tends to increase with decreasing $\sin\theta/\lambda$ [Fig. 3(a)]. It is also apparent from Fig. 3(b) that weak and intermediate reflections have a strong influence.

During the least-squares refinements, the hydrogen position parameters were kept fixed to the value obtained by the neutron data refinement, and the thermal parameters calculated from the $TLS+\phi_i$ tensors and internal contributions,[29] were also fixed. The T (translation), L (libration), and S (correlation) tensors, which describe the thermal agitation of the whole molecule, were obtained by least-squares refinement of the atomic Debye-Waller factor. The rotation ϕ_i describes libration between fragments of the molecule.

Given a set of correctly phased structure factors, integration may be performed directly in the crystal space without the intermediate of model functions. One of the electron properties dependent on the electron distribution may be defined by an operator equation:

$$\langle O\rangle=\int \hat{O}\rho(r)d^3r, \tag{3}$$

where the integration is performed over the volume of interest, which may be the whole crystal or a cell associated with a molecule, ion, or atom.

$\rho(r)$ is the FT of the structure factor phased by the multipolar model:

$$F(\vec{H})_{\text{mult}}=\sum_k P_{k,c}f_{k,\text{core}}(H)+P_{k,v}f_{k,\text{val}}\left(\frac{H}{\kappa_k}\right)+\sum_{l=0}^{4}\phi_{k,l}\left(\frac{H}{\kappa_k'}\right)\sum_{m=0}^{l}P_{k,lm\pm}Y_{k,lm\pm}\left(\frac{\vec{H}}{|H|}\right)\times T_k(\vec{H})\exp[i2\pi(\vec{H}\cdot\vec{r})]. \tag{4}$$

$\phi_{k,l}$ is the Fourier Bessel transform of $R_{k,l}$ of Eq. (2).

In the integration, we can indifferently make use of $|F_{\text{cal,mult}}|e^{i\phi_{\text{mult}}}$ or $|F_{\text{obs}}|e^{i\phi_{\text{mult}}}$ the module of these two quantities being almost identical (R factor $\sim$ 2%). Examples of properties of interest here are molecular dipole, quadrupole, and octupole outer moments, which depend on the inner part of the diffraction pattern, and are directly related to the definition of the integration volume. Definition of this volume is to some extent arbitrary, and the choice is analogous to the selection of density basis functions in the multipolar formalism. Acceptable volume partitioning must satisfy the conditions that $\Sigma_i v_i=V$ the volume of the cell, and $\Sigma_i q_i=0$, the unit cell must be neutral. In this study, results have been obtained by the so-called fuzzy or stockholder method,[30–32] and the discrete boundary partitioning.[33] More details about the structure, the electron density distribution, and the electrostatic properties of the molecule have been published elsewhere.[34]

THEORETICAL CALCULATIONS OF HYPERPOLARIZABILITY

The number of electrons in the molecule of NPP $C_{11}O_3N_2H_{14}$ (118e) preclude *ab initio* calculations. Since the nonlinear optical expansion coefficients are functions of linear optical properties, such as excitation energies and dipole matrix elements, the necessary electronic structure information can be conveniently obtained from a spectroscopically based semiempirical electronic structure description. The combination of the semiempirical modified neglect of differential overlap (MNDO) molecular orbital method[19] and the finite field technique[35,36] offers the avantage of allowing the simultaneous calculations of all appropriate tensor components of the polarizability (α) and of the first and second hyperpolarizabilities (β and γ) for large organic molecules with a moderate computational effort.

Values of β and γ have been obtained in the past for some monosubstituted benzenes[19] making use of symmetrical finite difference expressions, using the INDO method. In the electronic section of MOPAC (Ref. 18) (version 6.00), four approximated Hamiltonians are available: MNDO, MINDO/3, AM1, and PM3.

The energy of a molecule in an external field E may be expanded in a power series of the local field E as

$$W(E)=W(0)-\mu_{i0}E_i-\frac{1}{2!}\alpha_{ij}E_iE_j-\frac{1}{3!}\beta_{ijk}E_iE_jE_k$$

$$-\frac{1}{4!}\gamma_{ijkl}E_iE_jE_kE_L-\cdots, \tag{5}$$

where implicit summation over repeated indices is being assumed by convention. E_i is a component of the local field acting on the molecule, μ_{i0} is a component of the permanent dipole moment, α_{ij} is a tensor component of the polarizability, while β_{ijk} and γ_{ijkl} are components of the first and second order hyperpolarizability, respectively. If the molecule is considered to be in a uniform electric field aligned along the main axis of the system (i.e., $[E_{x,0,0}]$), the values of the polarizabilities along that axis $(\mu_{x0},\alpha_{xx},\beta_{xxx},\gamma_{xxxx})$ can be obtained. For this case, the energy expression reduces to

$$W(E_x)=W(0)-\mu_{i0}E_x-\frac{1}{2}\alpha_{xx}E_x^2-\frac{1}{6}\beta_{xxx}E_x^3-\frac{1}{24}\gamma_{xxxx}E_x^4$$

$$-\cdots. \tag{6}$$

Truncating this expression after the E^4 term and evaluating the energy at four field strengths $(\pm E_i,\ \pm 2E_i)$ leads to four equations with four unknowns. Similar expressions can be derived for ''nondiagonal'' tensor coefficients by the introduction of ''off-axis'' field interaction.

An alternate method for obtaining the polarizability and hyperpolarizabilities is to use the equation for the induced dipole moment instead of the energy; Both methods (the energy expansion and the dipole expansion) are implemented in the MOPAC program. Since the results based on self-consistent field calculations should be identical for both methods, this provides a good check on the results as to eventual numerical errors or configuration changes.

RESULTS AND DISCUSSIONS

The Unsöld approximation is a special case of the variational perturbation method in the form proposed by Dalgarno and Lewis[37] and Schwartz.[38] Its crucial point is that it permits calculation of both α and β from the knowledge of the exact ground-state function Ψ^0 only.

Following Boyd,[39] the linear polarizability is given by

$$\alpha_{ij}(\omega_p)=\frac{1}{\hbar}\sum_m\frac{\mu^i_{gm}\mu^j_{mg}}{(\omega_{mg}-\omega_p)}+\frac{\mu^j_{gm}\mu^i_{mg}}{(\omega^*_{mg}+\omega_p)}, \tag{7}$$

where m and g, respectively, label a virtual level and the ground-state wave functions, ω_{mg} is the transition frequency between level m and the ground-state g, ω_p is the frequency of the applied field.

For convenience let $\mu^i_{gm}=\langle g|\mu_i|m\rangle$ where μ is the dipole operator and $\hbar\omega_{mg}=\Omega_{mg}$, then Eq. (7) becomes

$$\alpha_{ij}(\omega_p)=\sum_m\langle g|\mu_i|m\rangle\langle m|\mu_j|g\rangle\frac{2\Omega_{mg}}{\Omega^2_{mg}-\Omega^2_p}$$

[assuming all quantities real in (7)]. Here, we consider only the diagonal components, so that

$$\alpha_{ii}(\omega_p)=\sum_m\frac{2\Omega_{mg}}{\Omega^2_{mg}-\Omega^2_p}|\langle g|\mu_i|m\rangle|^2.$$

Recall that

$$\sum_{m\neq g}\frac{2\Omega_{mg}}{\Omega^2_{mg}-\Omega^2_p}|\langle g|\mu_i|m\rangle|^2=\sum_m\frac{2\Omega_{mg}}{\Omega^2_{mg}-\Omega^2_p}|\langle g|\mu_i|m\rangle|^2-|\langle g|\mu_i|g\rangle|^2,$$

$$\alpha_{ii}(\omega_p)=\frac{2\Omega_{mg}}{\Omega^2_{mg}-\Omega^2_p}\left\langle g\left|\mu_i\sum_m\right|m\right\rangle\langle m|\mu_i|g\rangle-|\langle g|\mu_i|g\rangle|^2.$$

From the closure relation, we get

$$\alpha_{ii}(\omega_p)=\frac{2\Omega_{mg}}{\Omega^2_{mg}-\Omega^2_p}\langle g|\mu_i^2|g\rangle-\langle g|\mu_i|g\rangle^2,$$

$$\alpha_{ii}(\omega_p)=\frac{2\Omega_{mg}}{\Omega^2_{mg}-\Omega^2_p}=\langle g|\hat{\mu}_i^2|g\rangle,$$

where $\hat{\mu}_i=\mu_i-\langle g|\mu_i|g\rangle$. Assuming $\omega_p=0$ and looking only for the x component of the dipole moment, we get

$$\alpha_{xx}(\omega_p=0)=\frac{2e^2}{\Omega_{mg}}\langle g|\hat{x}^2|g\rangle.$$

According to the Unsöld[17] approximation, one replaces all the energy denominators by a common energy that is obtained from the Reiche-Thomas-Kuhn[40] sum rule:

$$\sum_{m\neq g}\frac{2m}{\hbar^2}\Omega_{mg}|\langle g|x|m\rangle|^2=1.$$

Assuming a single Ω_{mg} value leads to

$$\frac{1}{\Omega_x}=\frac{2m}{\hbar^2}|\langle g|\hat{x}^2|g\rangle|,$$

where Ω_{mg} has been replaced by Ω_x in order to feed the xx component of the polarizability α.

If we substitute this average value of the energy for Ω_{mg} in the equation giving α, we obtain

$$\alpha_{xx}(\omega=0)=2e^2\langle g|\hat{x}^2|g\rangle\frac{2m}{\hbar^2}\langle g|\hat{x}^2|g\rangle,$$

$$\alpha_{xx}(\omega=0)=\frac{4m}{\hbar^2}\langle g|e\hat{x}^2|g\rangle^2. \tag{8}$$

The linear polarizability depends then only on the quadrupole moment in the ground state. If the components of both the quadrupole and of the polarizability tensor are in 10^{-24} esu, the prefactor $4m/\hbar^2$ is equal to 7.98.

When the same method is applied to the nonlinear quadratic polarizability, similar results are obtained (see, for instance, Robinson[14]);

$$\beta_{xyz}(-\omega;\omega_1,\omega_2)$$

$$\simeq\left(\frac{e^3}{\hbar^2}\right)\frac{\Omega_x\Omega_y\Omega_z(\Omega_x+\Omega_y+\Omega_z)}{(\Omega_x^2-\omega^2)(\Omega_y^2-\omega_1^2)(\Omega_z^2-\omega_2^2)}\langle g|\hat{x}\hat{y}\hat{z}|g\rangle. \tag{9}$$

TABLE II. Column 1: labeling of the components of the properties. Column 2: dipole, polarizability, and hyperpolarizability calculated by the finite field method. Column 3: dipole, quadrupole, and octupole from the point charge model. Column 4: components of the dipole in D and diagonal values of α and β calculates, using Eqs. (8) and (10) in the text. (Unit systems are defined in each column, and a conversion factor is calculated in Appendix.)

	Dipole (eÅ)	Dipole (eÅ)	Dipole (D)
X	-1.51	-1.64	7.87
Y	-0.32	-0.366	-1.75
Z	0.10	0.017	0.08
	α tensor (D-24 esu)	Q_{ij} (eÅ^2)	α (D-24 esu) from Eq. (8)
XX	60.84	-4.67	174.0
YY	38.39	3.05	74.2
ZZ	14.95	1.10	9.6
XY	2.39	0.33	
XZ	-0.21	-0.48	
YZ	3.43	0.56	
	β tensor (D-30 esu)	O_{ijk} (eÅ^3)	β (D-30 esu) from Eq. (A1)
XXX	-24.90	-42.5	-8378.9
XYY	1.69	-5.3	
XZZ	0.03	-3.1	
YYY	1.23	-3.4	-285.9
YXX	-3.91	-8.9	
YZZ	0.16	-0.3	
ZZZ	-0.02	0.1	1.1
ZXX	-0.21	0.8	
ZYY	-0.09	0.2	

The calculations of the diagonal component β_{zzz} is reported in the Appendix [cf. Eq. (10)]. The prefactor between the diagonal components rises to 9.04, when octupolar moment and the β_{ijk} tensor are in 10^{-30} esu. The formula for off-diagonal components and more details will be published in a forthcoming paper.

It is interesting to check the validity of the Unsöld approximation, using the results obtained by a semiempirical method implemented, for instance, in the electronic part of MOPAC (AM1 Hamiltonian). From the semiempirical calculated atomic charges where the Cartesian coordinates of the atoms were referred to the inertial axis and the origin was taken at the center of mass of the molecule, we have calculated the dipole, the quadrupole, and the octupole of the NPP molecule. In the semiempirical MOPAC program, the atomic charges are obtained from a full Mulliken population analysis. Results of this so-called ''point charge model'' are listed in Table II together with the the polarizability and hyperpolarizability tensors calculated by the finite field method exposed previously and implemented in MOPAC.

We notice that the ratios between the diagonal elements of the polarizability tensor (in 10^{-24} esu) and those of the quadrupolar moment (in eÅ^2) are of the order of 13, while for the hyperpolarizability and the octupolar moment they range from 0.2 to 0.6. In the third column of Table II, diagonal components of polarizability and hyperpolarizability have been added, values were deduced from Eqs. (8) and (10), where the prefactor has been determined in both cases.

We observe a remarkable agreement between the relative order of magnitude of the diagonal components of the polarizability and hyperpolarizability tensors deduced from the finite field method, and those calculated from the multipolar moments of the ground-state charge distribution. However, the β tensor components calculated from the octupolar moment, are larger by two orders of magnitude with respect to those deduced by the finite field method. Clearly the assumption that the same energies should be used in α and in β is a questionable one.

This method however, indicated how the asymmetry and charge extension, reflected, respectively, in $\langle\hat{x}^3\rangle$ and $\langle\hat{x}^2\rangle$ are related to β. It is worthwhile to emphasize that the ratios between the diagonal tensors coefficients of β and O range from 0.2 to 0.6. The anisotropy is appearing between nonlinear quadratic hyperpolarizability and the octupolar ground-state charge distribution moment. Anyway, the largest value β_{xxx} along the charge transfer axis corresponds to the most important component O_{xxx}.

ELECTRONIC DENSITY DISTRIBUTION ANALYSIS

The results described in the previous section show that the Unsöld approximation gives relatively good values for α, but fall off by two orders of magnitude in the estimation of β. However, O'Hare and Hurst,[41] Flytzanis and Ducuing[15] have obtained more satisfactory results using the same model, respectively, on polar diatomic molecules and on

TABLE III. Net atomic charges $(+e)$ in NPP. (A) Fuzzy boundary partitioning of experimental density, (B) multipolar refinement. Also from semiempirical calculations using AM1 and PM3 Hamiltonians.

	A	*B*	AM1	PM3
C(1)	-0.07	0.20(1)	-0.20(6)	-0.51
C(2)	-0.02	-0.25(8)	-0.01(5)	0.06
C(3)	-0.09	-0.31(8)	-0.23(6)	-0.23
C(4)	0.03	0.10(1)	0.17(6)	0.05
C(5)	-0.18	-0.35(8)	-0.23(5)	-0.23
C(6)	-0.13	-0.39(9)	-0.01(5)	0.06
C(7)	-0.03	-0.40(1)	-0.01(9)	-0.10
C(8)	-0.08	-0.44(8)	-0.16(5)	-0.10
C(9)	-0.08	-0.45(7)	-0.17(5)	-0.11
C(10)	0.01	-0.51(6)	-0.02(5)	-0.08
C(11)	-0.10	-0.30(1)	-0.03(8)	0.05
N(1)	0.19	0.20(1)	0.55(7)	1.31
N(2)	-0.04	0.08(7)	-0.28(7)	0.08
O(1)	-0.18	-0.27(6)	-0.36(5)	-0.62
O(2)	-0.10	-0.20(6)	-0.37(5)	-0.63
O(3)	-0.19	-0.34(5)	-0.31(7)	-0.30
HC(2)	0.08	0.22(3)	0.16(3)	0.13
HC(3)	0.08	0.23(3)	0.13(2)	0.12
HC(5)	0.05	0.32(3)	0.14(3)	0.12
HC(6)	0.06	0.25(3)	0.16(3)	0.13
HC(7)	0.12	0.31(3)	0.10(2)	0.08
HC(8)	0.08	0.28(3)	0.09(2)	0.08
H'C(8)	0.01	0.23(3)	0.12(3)	0.06
HC(9)	0.04	0.23(3)	0.09(3)	0.06
H'C(9)	0.09	0.27(3)	0.10(3)	0.07
HC(10)	0.06	0.27(3)	0.10(3)	0.07
H'C(10)	0.09	0.28(3)	0.08(3)	0.06
HC(11)	0.06	0.27(3)	0.11(3)	0.07
H'C(11)	0.06	0.24(3)	0.07(3)	0.04
HO(3)	0.17	0.32(3)	0.20(3)	0.19

III-V semiconductors. Despite the discrepancies observed between the α and β values deduced from the theoretical point charge model and the finite field method, it is interesting to apply the same formalism to the multipolar molecular moments obtained from an electronic density study by x-ray diffraction. In this context, the molecular properties should reveal some intrinsic features about the bulk material, i.e., polarization trends, crystal effects, etc.

Using the Eq. (3) (Ref. 32) with $\hat{O} = 1$, $\vec{R}_{\alpha,i}$, $\vec{R}_{\alpha,i}\,\vec{R}_{\alpha,j}$, $\vec{R}_{\alpha,i}\,\vec{R}_{\alpha,j}\,\vec{R}_{\alpha,k}$, we have calculated, respectively, the charge, and the Cartesian components of the dipole, the quadrupole, and the octupole of the atoms and of the molecule. In the integration process, the multipolar phases, according to Eq. (4), were assigned to the structure factors. In noncentrosymmetric structures especially in a polar space group like $P2_1$, using the spherical approximation can produce dramatic errors in the evaluation of the electronic properties.

Table III lists the atomic charges derived from fuzzy boundary and multipolar methods, together with the values calculated from semiempirical methods using AM1 and PM3 Hamitonians MOPAC (version 6.00). The configuration of the molecule is that obtained from x-ray study.

Results obtained from experimental and theoretical methods agree on the strong negativity of the oxygen atoms, on the positive charge on the nitrogen atom N(1) and the hydrogen atom H(O_3) implied in an hydrogen bond. Results from AM1 Hamiltonian are very close to those derived from x-ray using the fuzzy boundary partitioning, the only sign difference is on the C(10) atom. Large negative charges on carbon atoms are offset by high positive charges of the attached hydrogen atoms. Most noteworthy is the complete agreement of the signs of the H atoms from theoretical and x-ray experimental results.

Comparison between the results from the different methods is easier if we examine a more global property like the molecular moment. The values of the molecular dipoles are in good agreement, however, we note differences in sign for the component Y between experimental and theoretical results (cf. Fig. 4). Such a variation in the orientation of the dipolar vector in the XY plane (inside the molecular mean plane) could be related to the molecular packing and the hydrogen bond in the crystal (cf. Table IV and Fig. 5).

Using Eq. (8) and the value of 7.98 of the prefactor, we have calculated the diagonal components of the polarizability tensor from the quadrupolar moments derived from experimental (x-ray) and theoretical (semiempirical point charge model) studies. To facilitate the comparison, those values

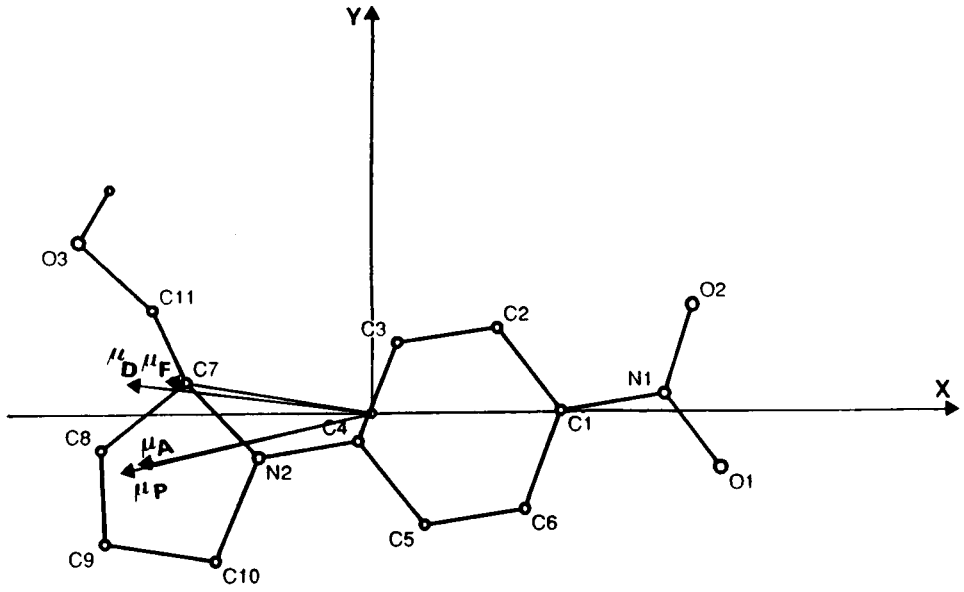

FIG. 4. Dipolar molecular moments calculated by different methods. The origin is at the center of mass of the molecule. The referential system is along the inertial axis. μ_P—dipole from the point charge model. μ_A—dipole from the AM1 (MOPAC). μ_D—dipole from the discrete boundary. μ_F—dipole from the fuzzy boundary.

with the quadrupolar moments and the polarizability deduced from the finite field method[35,36] are listed in Table V. The most remarkable feature between experimental values and those derived from the free molecule stands out in the α_{xx}, α_{yy}, and α_{xy} components. The experimental second moment component ($Q_{xx}<0$) shows a weaker charge expansion than in the free molecule along the X direction, while ($Q_{yy}>0$) implies a stronger contraction in the direction Y, i.e., towards the molecular axis X (cf. Fig. 4), with a more pronounced delocalization in the $\vec{x}+\vec{y}$ direction. According to the orientation of μ_D and μ_F (cf. Fig. 4), the electronic donating part of the molecule embedded in the crystal arises especially from the atoms of the chain involved in the hydrogen bond, whereas for the free molecule the dipole is directed towards the center of the five ring prolinol. In fact, the very efficient NLO properties of a free molecule computed by any software can be largely modified in the condensed matter.

From Eq. (A1) (cf. Appendix) and the value 9.04 of the prefactor, the same analysis has been conducted for the quadratic hyperpolarizability tensor components. Table VI lists the different values as previously defined for the case of the linear polarizability. As already mentioned for the α_{xx} component, we note a large underestimate of the β_{xxx} component, with respect to the value of the free molecule, which is partly compensated for, by a large value of β_{xxy} and β_{xyy}. Both the charge asymmetry and the charge extension have evolved differently in these two different states of the molecule. Our study reveals that β_{xxx} of the molecule in the crystal is not so large as predicted by semiempirical calculations, furthermore, the unidimensional character prevailing in the free molecule appears to be damped when the mol-

TABLE IV. Components of dipolar moment calculated from different methods. The origin coincides with the center of mass of the molecule, and the Cartesian coordinates refer to the inertial axes of the molecule.

	X	Y	Z	$\lvert\mu\rvert$ (D)
μ (Discrete boundary)	-1.60	0.194	0.446	8.0
μ (Fuzzy boundary)	-1.34	0.217	0.111	6.9
μ (AM1, MOPAC)	-1.51	-0.319	0.099	7.4
μ (PM3, MOPAC)	-1.53	-0.290	0.096	7.5
μ (Point charge model)	-1.64	-0.366	0.017	8.1

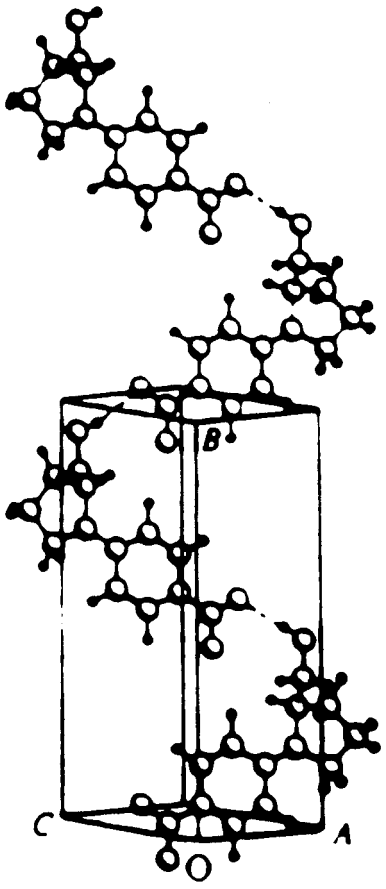

FIG. 5. Molecular packing in the NPP crystal. The hydrogen bond connects one oxygen atom of the nitro group of one molecule to the alcohol group of the next one.

TABLE V. Values of α from finite field AM1 and PM3 (D-24 esu) calculations are compared to the coefficients Q_{ij} of the quadrupolar moment (eÅ^2) derived from electronic density study. α_{ij} (D-24 esu) from Eq. (8) are added. The origin coincides with the center of mass of the molecule, and the Cartesian cooordinates refer to the inertial axes of the molecule.

α_{ij}	Discrete partition		Diffuse partition		Point charge model		Finite field method AM1	PM3
	Q_{ij}	α_{ij}	Q_{ij}	α_{ij}	Q_{ij}	α_{ij}		
α_{xx}	-1.82	26.4	-1.01	8.1	-4.67	174.0	60.84	57.32
α_{xy}	2.29		2.45		0.33		2.39	2.28
α_{xz}	-0.94		-0.81		-0.48		-0.21	0.12
α_{yy}	5.32	225.8	5.14	210.8	3.05	74.2	38.39	35.25
α_{yz}	0.62		0.60		0.56		3.43	3.21
α_{zz}	2.63	55.2	2.71	58.6	1.10	9.6	14.95	14.01

ecule is embedded in a crystal.

In the course of our investigations, we observe that the part of the first, second atomic moments included in the molecular quadrupolar moment, as the part of the first, second, and third atomic moments included in the molecular octupole are not negligible, and intervene for about 30% in the molecular properties. Those features are certainly in relation with the molecular interactions, which screen to some extent the nonlinear efficiency of the molecule. It is a domain that has not been really explored as the x-ray data has not presently reached the necessary accuracy to evidence such phenomena.

CONCLUSIONS

We have shown, in this study, that there is reasonable agreement between electronic properties deduced from x-ray diffraction and those from semiempirical calculations, using the point charge model (molecular dipole, etc.). There is no doubt about the relation between the ground-state molecular quadrupole and octupole and the polarizability of the molecule.

Through the so-called ''point charge model,'' it is possible to follow the appearance of the discrepancies between the concerned electronic moments and the semiempirical calculated polarizabilities. As we have shown, the Unsöld approximation gives relatively good results for α, but falls off by two orders of magnitude in the estimation of β. We observe however, that the components of the octupolar moment from the point charge model roughly parallel the values of the hyperpolarizability tensor with some inconsistency in sign, especially when the values are weak. Concerning the results from the experimental electronic density study, there are still some added fluctuations in the modulus of the components with respect to those derived from the so-called ''point charge model,'' but the signs are all in good agreement.

We intend to apply the same technique to the calculation of the macroscopic properties χ of the crystal, which could be a very convenient and general method for the estimation of net SHG efficiency of organic crystals.

As the components of the α tensor seem to be determined more accurately, we will project calculations of the dielectric constants and values of the refraction indices using a Sellmeier type formula, and the results could be compared to those derived from experimental measurements. Investigations of this type are currently carried on with complex crystals built up from anions and

TABLE VI. Values of β from finite field AM1 and PM3 (10^{-30} esu) calculations are compared to the coefficients O_{ijk} of the octupolar moment (eÅ^3) derived from electronic density study. β_{ijk} (10^{-30} esu) from Eq. (A1) are added. The origin coincides with the center of mass of the molecule, and the Cartesian cooordinates refer to the inertial axes of the molecule.

β_{ijk}	Discrete partition		Diffuse partition		Point charge model		Finite field method AM1	PM3
	O_{ijk}	β_{ijk}	O_{ijk}	β_{ijk}	O_{ijk}	β_{ijk}		
β_{xxx}	-26.49	-793.2	-21.23	-195.8	-42.50	-8378.9	-24.90	-23.55
β_{xxy}	-5.95		-5.22		-8.93		-3.91	-3.93
β_{xxz}	2.85		2.65		0.875		-0.21	-0.37
β_{xyy}	-10.33		-9.05		-5.27		1.69	2.09
β_{xyz}	-1.69		-1.53		-0.69			
β_{xzz}	-4.88		-4.75		-3.09		0.03	0.06
β_{yyy}	-2.07	-529.6	-2.09	-501.1	-3.36	-285.9	1.23	1.25
β_{yyz}	1.79		1.73		0.22		-0.09	-0.06
β_{yzz}	-0.76		-0.73		-0.27		0.16	0.15
β_{zzz}	1.30	81.8	1.29	66.4	0.08	1.1	-0.02	-0.05

cations the 2-amino-5-nitropyridinium-dihydrogenphosphate (2A5NPDP) and the 2-amino-5-nitropyridinium-*L*-monohydrogentartrate (2A5NPLT). Our preliminary results on these compounds should indicate that the Unsöld approximation is no more valid when we are dealing with inorganic anions (e.g., $PO_4H_2^-$). Is the ionique structure or the size of the system responsible for the failure of the model? We are pursuing further investigations to elucidate the shortcomings of the model. Getting information on the role of the crystal field is also a very interesting topic we would like to explore.

APPENDIX

We start from the formula of Robinson,[14] Eq. (9) in the text where Ω refers to the frequency and not to the energy. We consider only the diagonal component, for instance; β_{zzz} and substitute Ω by ω for the frequency. We assume that the input and output frequencies are 0:

$$\beta_{zzz}(\omega=0)=\frac{e^3}{\hbar^2}\frac{\omega_z^3(3\omega_z)}{\omega_z^6}\langle g|\hat{z}^3|g\rangle,$$

$$\beta_{zzz}(\omega=0)=\frac{e^3}{\hbar^2}\frac{3}{\omega_z^2}\langle g|\hat{z}^3|g\rangle,$$

$$\beta_{zzz}(\omega=0)=\frac{e^3}{\Omega_z^2}\langle g|\hat{z}^3|g\rangle,$$

where we have replaced $\hbar\omega_z$ by the energy Ω_z. Now we apply the result of the Reiche-Thomas-Kuhn sum rule leading to

$$\frac{1}{\Omega_z}=\frac{2m}{\hbar^2}\langle g|\hat{z}^2|g\rangle.$$

Elimination of Ω_z between the two previous equations leads to

$$\beta_{zzz}(\omega=0)=3e^3\left(\frac{2m}{\hbar^2}\right)^2\langle g|\hat{z}^2|g\rangle^2\langle g|\hat{z}^3|g\rangle,$$

and, finally,

$$\beta_{zzz}(\omega=0)=\frac{12m^2}{\hbar^4}(\langle g|e\hat{z}^2|g\rangle)^2\langle g|e\hat{z}^3|g\rangle. \qquad \text{(A1)}$$

If we express β_{zzz} in 10^{-30} esu, then as the multipolar moments (quadrupole and octupole) have been calculated, respectively, in $e\text{Å}^2$ and $e\text{Å}^3$, the conversion prefactor has to be

$$12\,\frac{(9.1\times10^{-28})^2(4.8\times10^{-10}\times10^{-16})^2(4.8\times10^{-10}\times10^{-24})}{(1.05\times10^{-27})^4}$$

$$=9.0410^{-30}.$$

*Author to whom correspondence should be addressed.

[1] D.S. Chemla and J. Zyss, *Nonlinear Optical Properties of Organic Molecules and Crystals* (Academic Press, New York, 1987), Vols. 1 and 2

[2] C.W. Drick, R.J. Twieg, and G. Wagniere, J. Am. Chem. Soc. **108**, 5387 (1986).

[3] D. Li, T.J. Marks, and M.A. Ratner, Chem. Phys. Lett. **131**, 370 (1986).

[4] D.-Q. Li, M.A. Ratner, and T.J. Marks, J. Am. Chem. Soc. **110**, 1707 (1988).

[5] V.J. Docherty, D. Pugh, and J.O. Morley, J. Chem. Soc. Faraday Trans. **2**, 81 (1985); **2**, 1179 (1985).

[6] J.O. Morley, V.J. Docherty, and D. Pugh, J. Chem. Soc. Perkin Trans. II **1987**, 1351; **1987**, 1357; **1987**, 1361.

[7] J.O. Morley, J. Chem. Soc. Perkin Trans. II **1989**, 103.

[8] Y. Itoh, K. Oono, M. Isogai, and A. Kakuta, Mol. Cryst. Liq. Cryst. **170**, 259 (1989).

[9] K. Ohno, Y. Itoh, T. Hamada, M. Isogai, and A. Kakuta, Mol. Cryst. Liq. Cryst. A **182**, 17 (1990).

[10] A. Ulman, J. Phys Chem. **92**, 2385 (1988).

[11] J. Zyss and G. Berthier, J. Chem. Phys. **77**, 3635 (1982).

[12] M. Nakano, K. Yamagichi, and T. Fueno, *Nonlinear Optics of Organics and Semiconductors*, Springer Proceedings in Physics Vol. 36 (Springer-Verlag, Berlin, 1988), pp. 98–106.

[13] Y. Itoh, T. Hamada, A. Kakuta, and A. Mukoh, Proc. SPIE **293**, 1337 (1990).

[14] F.N.H. Robinson, Bell Syst. Tech. J. **46**, 913 (1967).

[15] Chr. Flytzanis and J. Ducuing, Phys. Rev. **178**, 1218 (1968).

[16] S.S. Jha and N. Bloembergen, Phys. Rev. **171**, 891 (1968).

[17] A. Unsöld, Z. Phys. **43**, 388 (1927).

[18] J.J. Stewart, Computer Code MOPAC, Version 6.00 (MVS version), Frank J. Seiler Research Laboratory, U.S. Air Force Academy, Colorado Springs, CO, 1990.

[19] J. Zyss, J. Chem. Phys. **70**, 3333 (1979); **70**, 3341 (1979), Parts I and II.

[20] R.F. Stewart, J. Chem. Phys. **58**, 1668 (1973).

[21] P. Coppens, T.N. Guru Row, P. Leung, E.D. Stevens, P.J. Becker, and Y.W. Yang, Acta Crystallogr. Sec. A **35**, 63 (1979).

[22] M. Souhassou, C. Lecomte, R.H. Blessing, A. Aubry, M.M. Rohmer, R. Wiest, M. Benard, and M. Marraud, Acta. Crystallogr. B **47**, 253 (1991).

[23] J. Zyss, J.F. Nicoud, and M. Coquillay, J. Chem. Phys. **81**, 4160 (1984).

[24] A. Perigaud, F. Gonzales, and M. Cunisse, Ann. Chim. Fr. **16**, 133 (1991).

[25] P. Andreazza, D. Josse, F. Lefaucheux, M.C. Robert, and J. Zyss, Phys. Rev. B **45**, 7640 (1992).

[26] R.H. Blessing, J. Appl. Crystallogr. **22**, 396 (1989), and references cited therein.

[27] Reactor ORPHEE, Laboratoire Leon Brillouin CEN Saclay, France.

[28] N. Hansen and P. Coppens, Acta. Crystallogr. Sec. A **34**, 909 (1978).

[29] F. Baert, P. Schweiss, G. Heger, and M. More, J. Mol. Struct. **29**, 178 (1988).

[30] F.L. Hirshfeld, Acta. Crystallogr. Sec. A **32**, 239 (1976).

[31] F.L. Hirshfeld, Theor. Chim. Acta. **44**, 129 (1977).

[32] P. Coppens, G. Moss, and N. Hansen (unpublished).

[33] P. Coppens, Phys. Rev. Lett. **34**, 98 (1975).

[34] A. Fkyerat, A. Guelzim, F. Baert, W. Paulus, G. Heger, J. Zyss,

and A. Perigaud, Acta. Crystallogr. Sec. B **51**, 197 (1995).
[35] K.D. Singer and A.F. Garito, J. Chem. Phys. **75**, 3572 (1981).
[36] H.A. Kurtz, J.J.P. Stewart and K.M. Dieter, J. Comp. Chem. **11**, 82 (1990).
[37] A. Dalgarno and J. Lewis, Proc. R. Soc. London Ser. A **233**, 70 (1956).
[38] C. Schwartz, Ann. Phys. (N.Y.) **6**, 156 (1959).
[39] R.W. Boyd, *Nonlinear Optics* (Academic, New York, 1992).
[40] F. Reiche and W. Thomas, Naturwissenschaften **13**, 627 (1925); W. Kuhn, Z. Phys. **33**, 408 (1925).
[41] J.M. O'Hare and R.P. Hurst, J. Chem. Phys. **46**, 2356 (1967).